Neuron, Volume *83*

Supplemental Information

Multisensory Integration in the Mouse Striatum

Ramon Reig and Gilad Silberberg

Supplemental Information includes:

Figures S1-S7

Supplemental Experimental Procedures

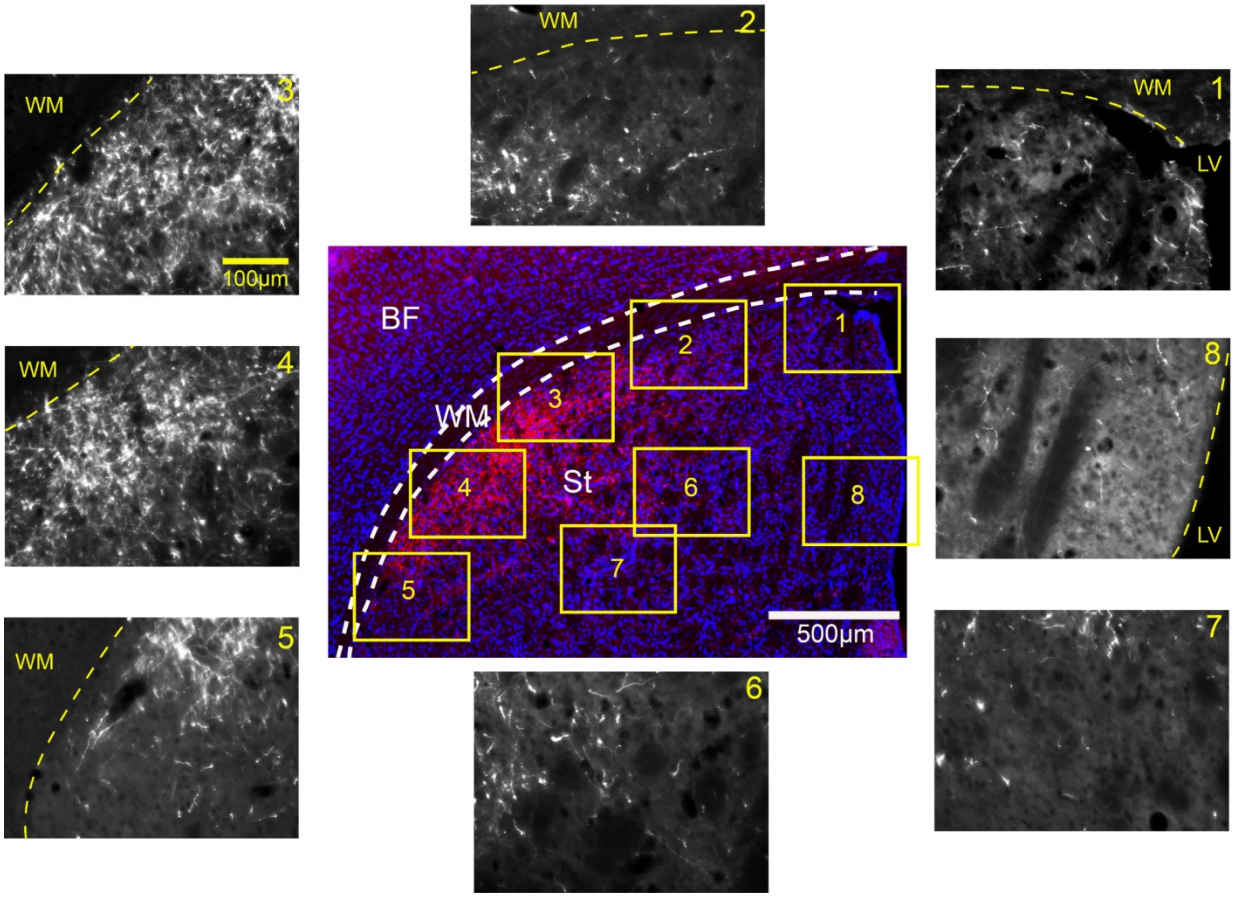

Figure S1. Ipsilateral axonal projections from cortical S1 to dorsal striatum (related to figure 1). Anterograde tracing from layer 5 in cortical S1 (barrel field - BF) to dorsal striatum (center image). Insets 1-8 show higher magnification of axonal projections (in white) throughout dorsal striatum. Note the sparse labeling of cortical axons in dorsomedial striatum (inset 1) compared to the dense labeling in dorsolateral striatum (insets 3-5).

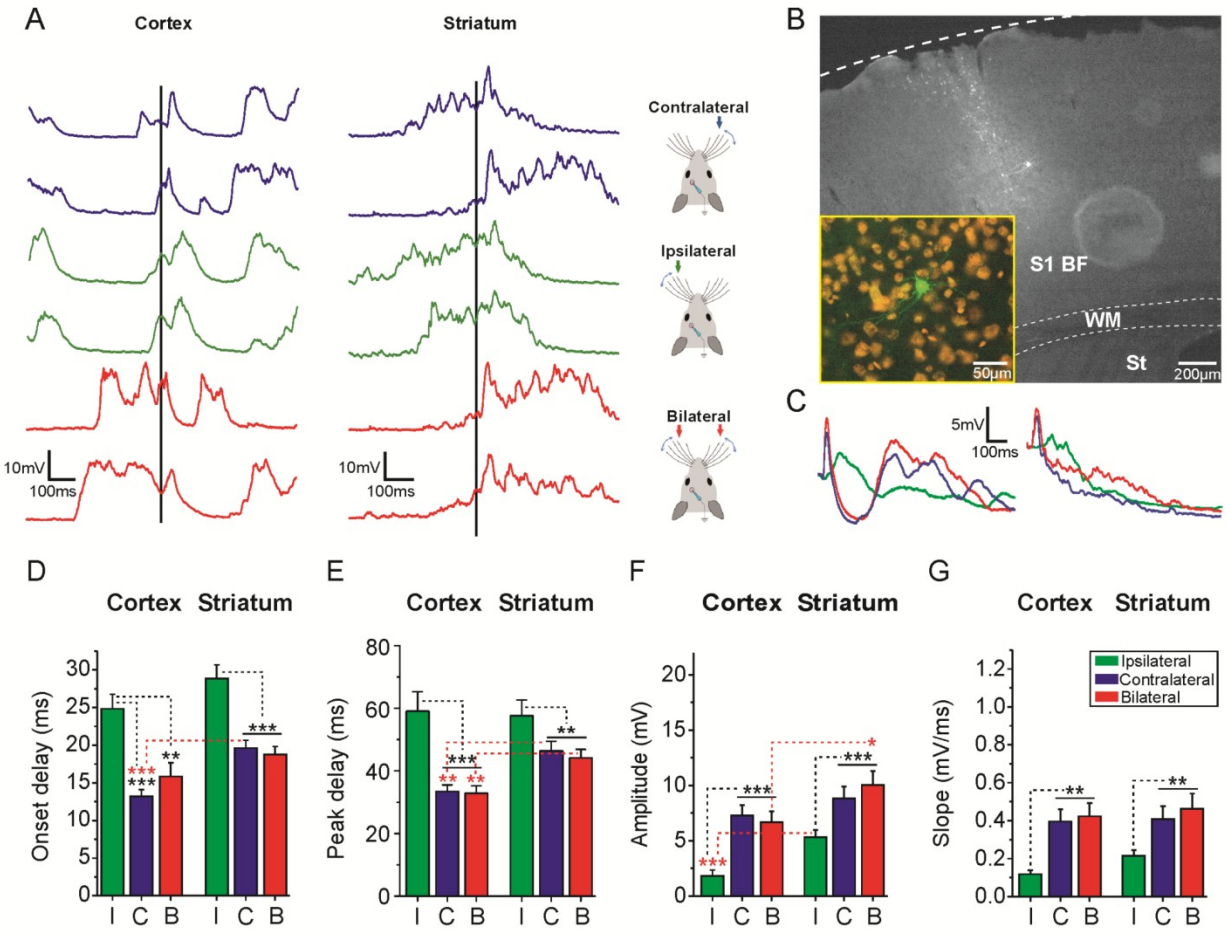

Figure S2. Responses to bilateral whisker deflection in cortical and striatal MSNs during up states (related to Figure 1). A. Example of responses to whisker deflection in a cortical pyramidal neuron (left) and a striatal MSN (right) during up states. **B.** Morphological reconstruction of the pyramidal cortical neuron recorded in A. **C.** Waveform average of the responses for the neurons showed in A. **D-G**. Average responses of cortical and striatal neurons to whisker deflection during up states. Ipsilateral in green, contralateral in blue, and bilateral stimulation in red. Onset delay (D), peak delay (E), amplitude (F), and slope (G). Scales are the same as in Figure 1F-I for comparison of up and down states. Cortical neurons n = 17, striatal MSN n = 20. Error bars represent the standard error of the mean (SEM) and asterisks *, **, *** represent p values smaller than 0.05, 0.01, 0.001, respectively.

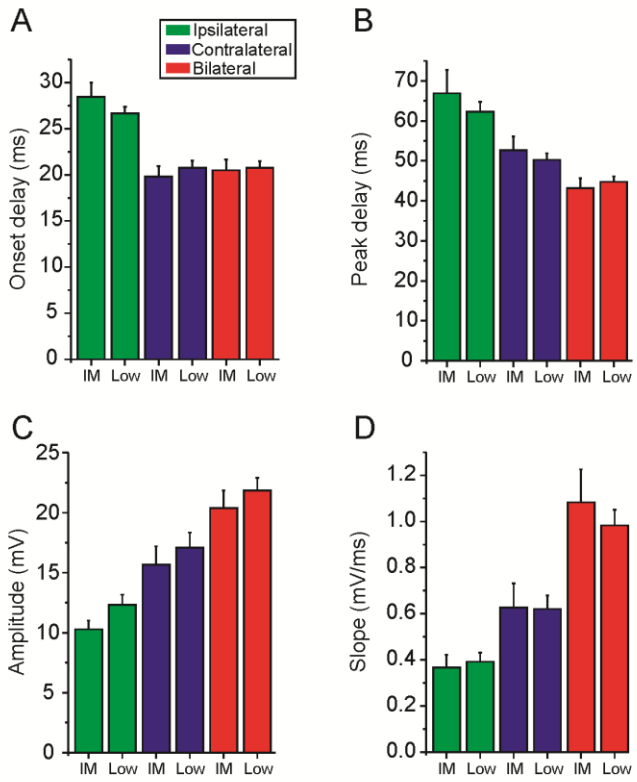

Figure S3. High vs. low chloride intracellular solution in dorsolateral MSNs (related to Figure 2). Average responses of dorsolateral striatal MSNs recorded with Intermediate Cl^- (30 mM, "IM") and Low Cl^- (10 mM, "Low") intracellular solution. Ipsilateral in green, contralateral in blue, and bilateral stimulation in red. Onset delay (A), peak delay (B), amplitude (C), and slope (D). No significant differences were observed between MSNs recorded with intermediate and low chloride solutions, for any of the presented measurements. IM MSNs n = 20, Low MSNs n = 28. Error bars represent the standard error of the mean (SEM).

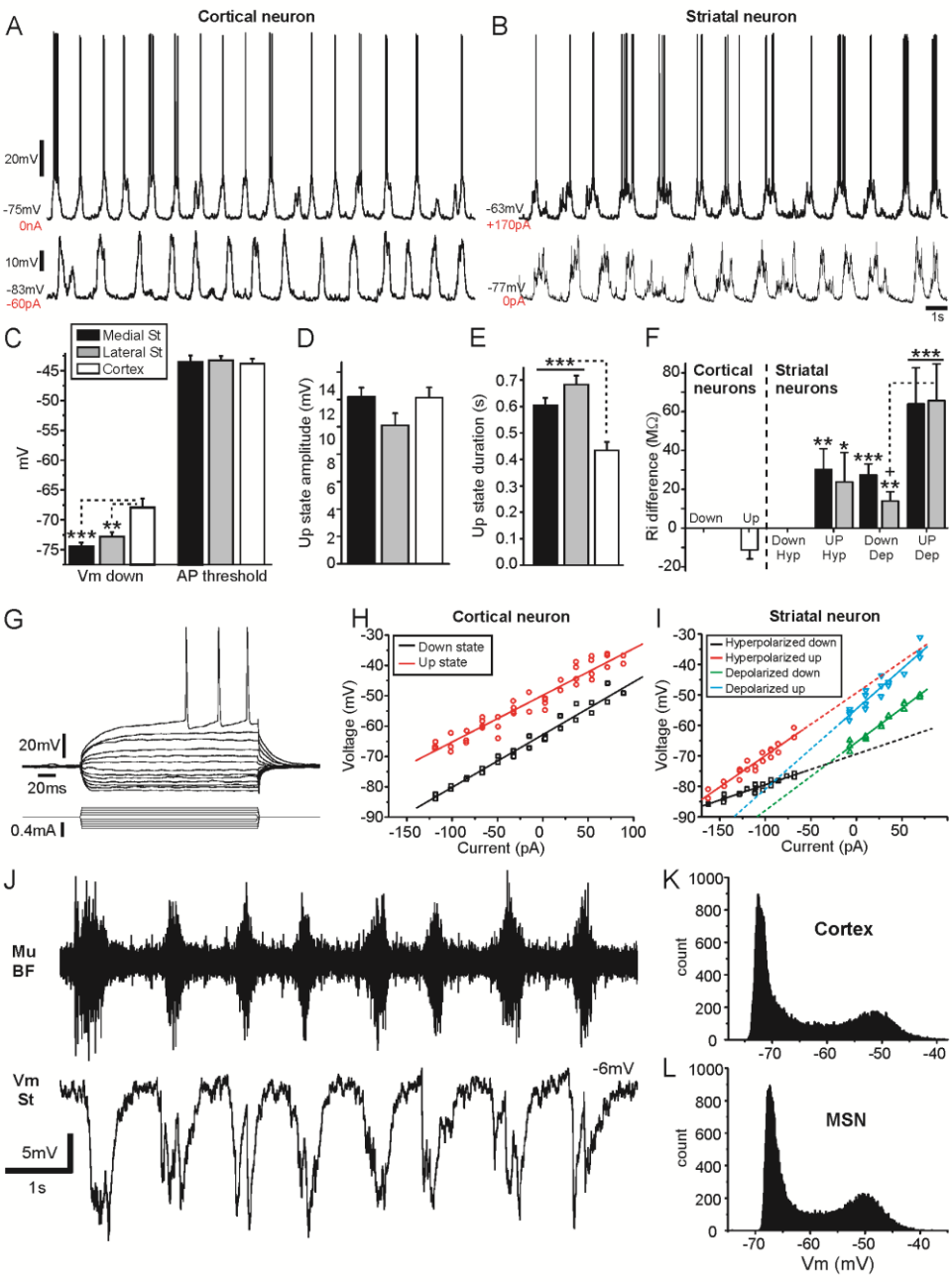

Figure S4. Intrinsic properties and spontaneous activity of cortical and striatal neurons (related to Figures 1 and 2). A-B. Examples of whole-cell patch clamp recordings of spontaneous slow oscillations in cortical and striatal neurons at different holding potentials. Note that at resting membrane potential (0 pA, as shown in red) the cortical but not striatal neuron discharges action potentials during up states. **C-E**. Properties of spontaneous slow oscillations in cortical pyramidal cells and striatal MSNs recorded in dorsomedial (medial St) and dorsolateral (Lateral St). Membrane potential (Vm) during down states and action potential threshold (C). Up state amplitude (D). Up state duration (E). **F**. Changes in the input

resistance of cortical and striatal neurons during up and down states. In MSNs, input resistances were different when extracted from hyperpolarizing and depolarizing current steps due to inward rectification by Kir channels. **G**. Example of current injections steps in a striatal MSN. **H-I**. Examples of current/voltage plots for cortical (H) and striatal (I) neurons, using depolarizing and hyperpolarizing current steps at Down- and UP states. Cortical neurons n = 17, dorsomedial MSNs n = 24, dorsolateral MSNs n = 20. Error bars represent the standard error of the mean (SEM) and asterisks *, **, *** represent p values smaller than 0.05, 0.01, 0.001, respectively. In F, asterisks represent comparison to the "Down Hyperpolarized" condition while "+" represents the comparison with the "UP depolarized" condition. **J.** MSNs receive inhibitory inputs during up states, as seen in the simultaneous extracellular recording in ipsilateral barrel cortex (top trace) and whole-cell recording in a striatal neuron (bottom trace). The recorded neuron was depolarized to the excitatory reversal potential in order to reveal inhibitory voltage responses. **K-L**. Bimodal distribution of membrane potential during spontaneous activity. Examples of bimodal membrane potential distribution of a cortical layer 5 pyramidal neuron (barrel cortex (K)) and a striatal MSN (L).

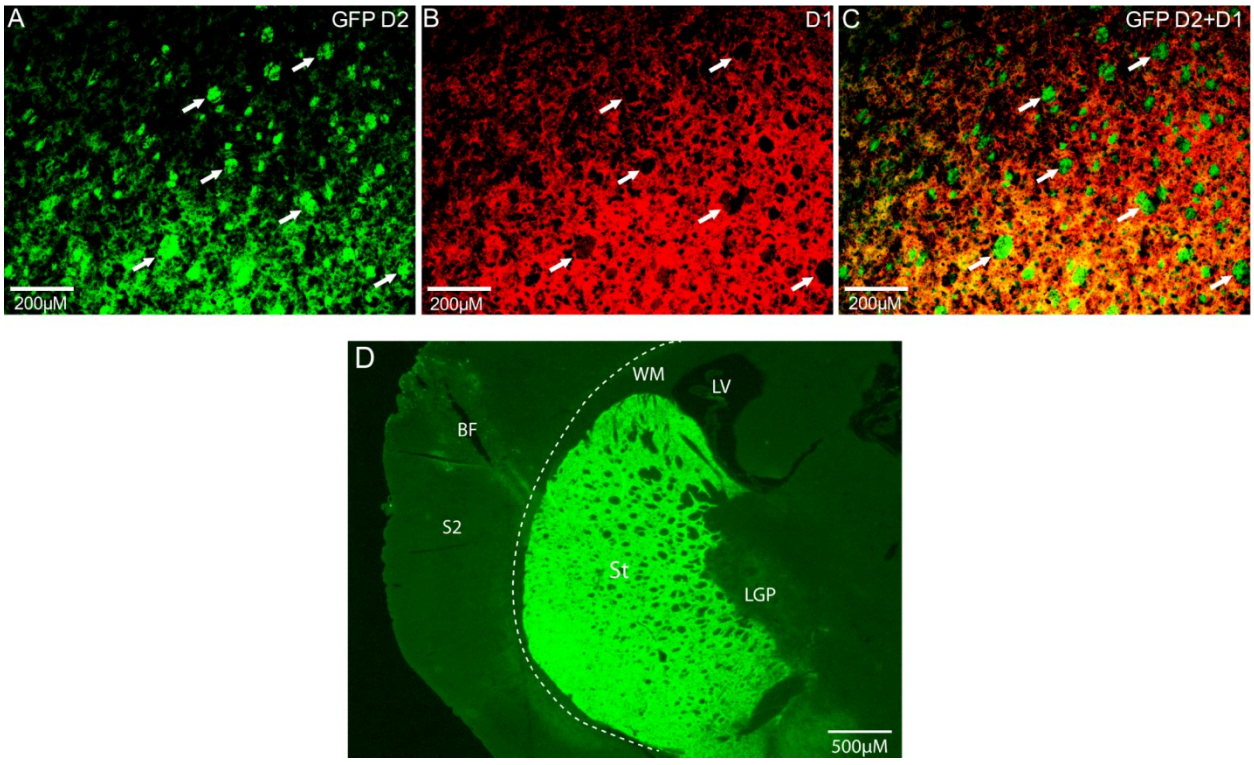

Figure S5. Control experiment showing D1 antibody staining of a slice from a Drd2 BAC transgenic mouse. A-C (related to Figure 5). The arrows point at 6 examples of D2-EGFP positive neurons from a Drd2-BAC transgenic mouse (Gong et al., 2003), all of which are not stained by the D1 antibody, as also evident in the merged image (*right panel*). **D**. Example of D1 inmunostaining in a wild-type mouse, highlighting the strong D1 expression throughout striatum.

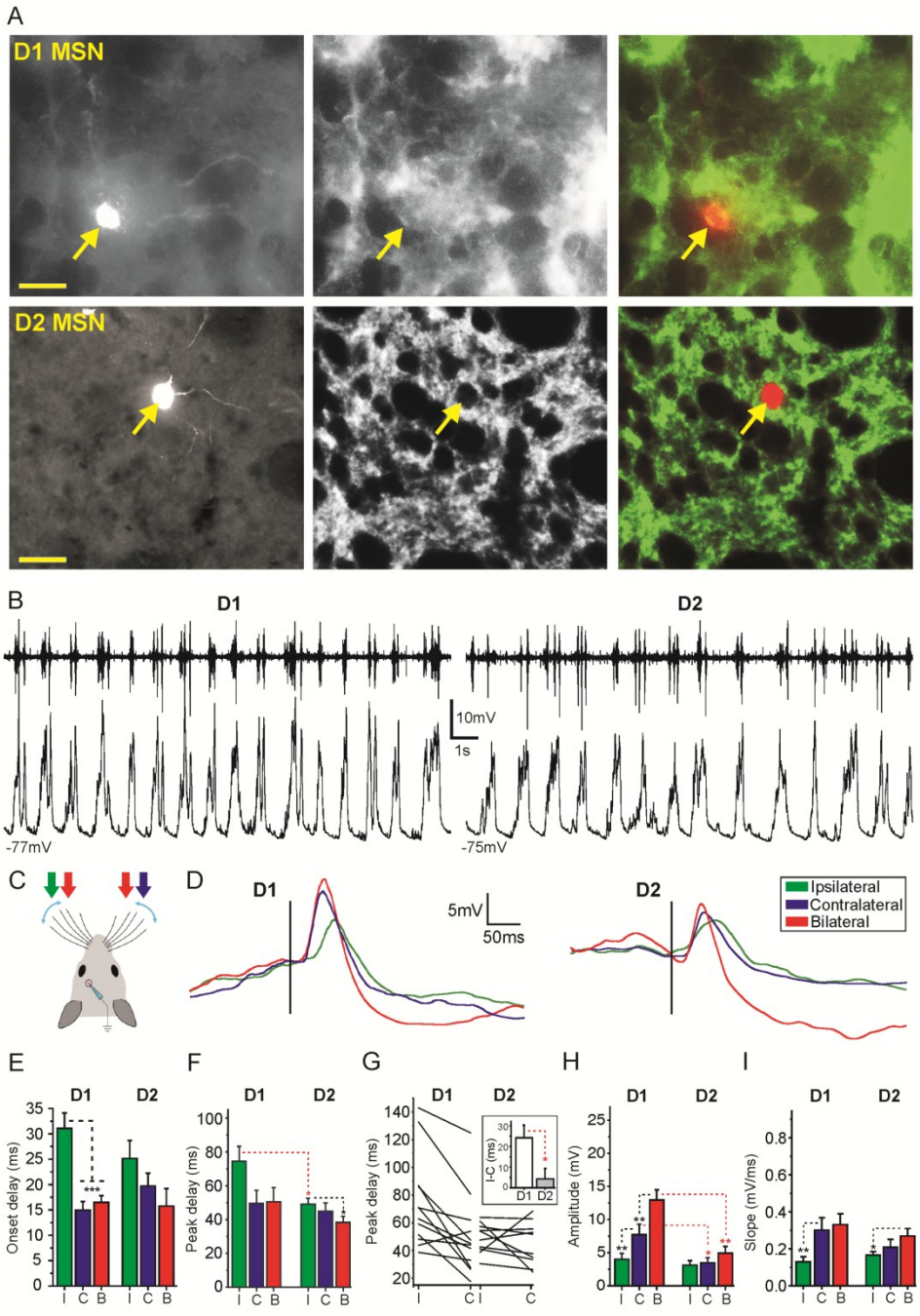

Figure S6. Direct and indirect pathway MSNs responding to bilateral whisker deflection during up states (related to figure 5). A. Examples of inmunohistochemestry for identifying D1 and putative D2 MSNs. From left to right; Neurons filled with neurobiotin, D1 receptor expression, and merged images of neurobiotin (red) and D1 receptor expression (green). Yellow narrows indicate the corresponding neuron position in the respective images **B**. Raw traces of whole cell recordings in D1 (left) and D2 (right) MSNs (bottom traces) and simultaneous extracellular recordings in ipsilateral BF (top traces) during

spontaneous slow oscillations. **C**. A schematic of the whisker stimulation procedure. **D.** Waveform averages of responses to whisker deflections in D1 MSN (left) and D2 MSN (right). **E-F**, **H-I**. Averages comparing the responses for contralateral (blue), ipsilateral (green) and bilateral stimulation (red) in D1 and D2 MSNs during up states. (E) Average onset delays, (F) Peak delays, (I) slopes (D1 MSN = 12; D2 MSN = 10), (H) amplitudes (D1 MSN = 15; D2 MSN = 13, we consider 0mV amplitude when responses were not clear detectable as in the cases of E, F, I, and G). **G**. Peak delays for all D1 and D2 subpopulations in response to contralateral and ipsilateral stimuli. Inset shows the time difference between the peak of the ipsilateral and contralateral responses for D1 and D2 MSNs. Error bars represent the standard error of the mean (SEM) and asterisks *, **, *** represent p values smaller than 0.05, 0.01, 0.001, respectively.

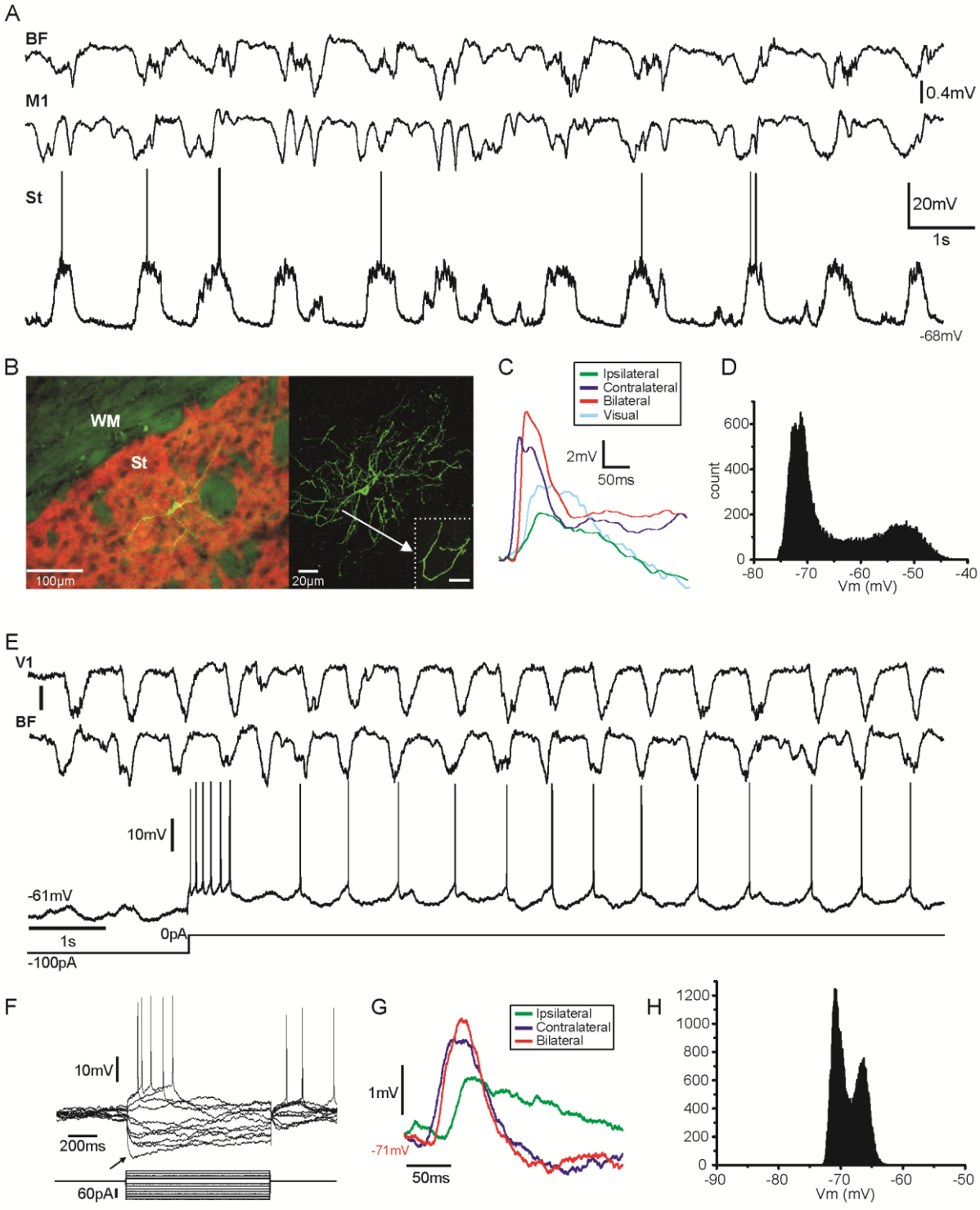

I

	Neuron properties			Onset delay (ms)			Amplitude (mV)			Slope (mV/ms)		
	AP duration (ms)	Vm (mV)	Up states amplitude (mV)	Contra	Ipsi	Bilateral	Contra	Ipsi	Bilateral	Contra	Ipsi	Bilateral
FS1	0.86	-75	15.65	21.15	35.2	31.7	12.35	6.98	14.38	0.73	0.1	0.9
FS2	0.8	-69	11.74	12.86	42.6	9.4	4.65	4.3	7.37	0.12	0.14	0.21
ChI1	1.58	-47.5	6.16	33.2	46.2	34.1	1.8	1.09	2.26	0.074	0.045	0.098
ChI2	1.28	-49.6	5.81	31.7	45.8	30.7	2.49	2.18	2.58	0.067	0.039	0.071

Figure S7. *In vivo* whole cell recordings from striatal interneurons. **A-D. Fast spiking interneuron (related to Figures 2 and 5). A**. An example of simultaneous whole-cell recording from a fast spiking interneuron and dual extracellular recordings in ipsilateral BF and M1 during spontaneous activity. **B**. Fluorescent image (left) and confocal reconstruction (right) of the same interneuron. The inset shows the smooth (aspiny) dendrites. **C**. Waveform average of the interneuron responses to visual stimulation (light blue trace) and ipsilateral (green trace), contralateral (dark blue trace), and bilateral (red trace) whisker deflection. **D**. Bimodal distribution of membrane potential during spontaneous activity. **E-H. Cholinergic interneurons**. **E.** An example of simultaneous whole-cell recording from a cholinergic interneuron and dual extracellular recordings in BF and V1 during spontaneous activity. Note than when the interneuron is not hyperpolarized by negative holding current, it discharges action potentials in synchrony with the cortical up states (negative peaks in the LFP recording). The scale bar for local field potentials is 0.4 mV. **F.** Response of the same cholinergic interneuron to step current injections. Note the voltage sag response (arrow) and rebound spikes characteristic for cholinergic interneurons. **G**. Waveform average of responses to bilateral whisker deflections at hyperpolarized holding potential. **H**. Bimodal distribution of membrane potential during spontaneous activity. **I. Intrinsic properties and responses to bilateral whisker stimulation recorded in striatal interneurons.** Amplitudes of up states and tactile responses were measured at resting membrane potential for FS interneurons and around -70 mV for cholinergic interneurons, during down states.

Experimental Procedures

Ethical approval.

All experiments were performed according to the guidelines of the Stockholm municipal committee for animal experiments.

Electrophysiological recordings.

Adult C57BL6 mice of both sexes between 2-6 months of age were used to perform the experiments (n = 92). Anesthesia was induced by intraperitoneal injection of ketamine (75 mg/kg) and medetomidine (1 mg/kg) diluted in 0.9 % NaCl. A maintaining dose of ketamine (30 mg/kg i.m.) was administrated every 2 hours or after changes in the EEG or reflex responds to paw pinches. Animals were sacrificed after

recordings by receiving an overdose of sodium pentobarbital (200 mg/kg I.P.). Tracheotomy was performed to increase mechanical stability during recordings by decreasing breathing related movements. Mice were placed in a stereotaxic device and air enriched with oxygen was delivered through a thin tube placed 1 cm from the tracheal cannula. Temperature was maintained between 36-37.5 °C using a feedback-controlled heating pad (FHC Inc.). Craniotomies were made at 5 sites for patch clamp and extracellular recordings: AP 0 mm from Bregma, L 2.5 mm (dorsomedial striatum); AP 0 mm from Bregma, L 3.75 mm (dorsolateral striatum); AP -1.5 mm, L 3.25 mm (S1); AP 1.5 mm, L 2 mm (M1); AP -3.5 mm, L 2.5 mm (V1) (following Paxinos and Franklin (2001)).

Whole-cell recordings were obtained from dorsolateral striatum between 1854-2613 µm deep and in layer V of cortical barrel field between 617-863 µm from the pia, in a perpendicular penetration angle (30°-40°). Signals were amplified using MultiClamp 700B amplifier (Molecular Devices) and digitized at 20 KHz with a CED acquisition board and Spike 2 software (Cambridge Electronic Design). Patch pipettes were pulled with a Flaming/Brown micropipette puller P-87 (Sutter Instruments) and had an initial resistance of 5-12 MΩ, with longer tips than the standard ones to minimize cortical damage. Pipettes were back-filled with intracellular solution containing the following (in mM): 125 K-gluconate, 10 KCl, 10 Na-Phosphocreatine, 10 HEPES, 4 ATP-Mg, 0.3 GTP-Na. A subset of experiments was performed with intracellular solution containing 105 K-gluconate, 30 KCl, 10 Na-Phosphocreatine, 10 HEPES, 4 ATP-Mg, 0.3 GTP-Na. Response latencies and amplitudes to whisker stimulation were not different across experiments performed with either intracellular solution (Figure S3).

Extracellular recordings were obtained using tungsten electrodes with impedances of 1-2 MΩ. The electrodes were placed in infragranular layers in somatosensory (BF), motor (M1), and visual (V1) cortex with an angle between 15° and 25°. Recordings were amplified using a Differential AC Amplifier model 1700 (A-M Systems) and digitized at 10 KHz with CED and Spike-2 simultaneously with the whole-cell recording.

Stimulation protocols.

Whisker stimulation was obtained by brief air puffs delivered by a picospritzer unit (Picospritzer III, Parker Hannifin, NJ) via 1 mm diameter plastic tubes placed at ~20 mm in front of the whiskers of both sides. Air puffs (15 ms duration) were given at least 40 times for each stimulus condition (ipsilateral, contralateral, or bilateral stimulation) in a random order, with 5 seconds of inter-stimulus interval. Air pressure was equal in both sides (20 p.s.i.) and evoked synaptic responses when stimulating the

contralateral and ipsilateral whisker. The whisker displacement following air puff was monitored and was determined to occur 11.0 ± 0.1 (n = 3 animals) ms following the trigger command. The reference onset time for the stimulus was therefore determined as 11 ms following the computer trigger command for the air puff.

Visual stimulation was delivered by a white LED positioned 50 mm from the contralateral eye. Stimulus duration was 10 ms and was delivered with interstimulus intervals of at least 5 seconds. The eye was covered with Vaseline in order to prevent drying, as previously described (Holtmaat et al., 2009). Visual responses were confirmed by monitoring the activation of the contralateral visual cortex using extracellular recordings (Figure 3F,G).

Multisensory stimulation. Tactile and visual stimuli were delivered using the same protocols as described above. In a subset of experiment we delivered the whisker stimulation with different delays with respect to the visual stimulus. Specifically, whisker stimulation was delivered in 5 different conditions; 1. Independently, using only contralateral whisker stimulation. 2. Simultaneously triggered with visual stimulation. 3. At the same time as the onset of the visual responses. 4. In synchronization with the peak of the visual response. 5. One second after visual responses. The response onset and peak were obtained independently for each modality and then used in the multisensory stimulation protocols.

Analysis.

Up and Down states were extracted from membrane potential recordings using an algorithm described by Seamari and colleagues (Seamari et al., 2007). Sensory responses were classified according to those occurring during “Up” or “Down” states, including cases in which sensory stimulation triggered state transitions (Reig and Sanchez-Vives, 2007). Stimuli were given at regular intervals (0.2 Hz) and therefore the probability that they occurred at different periods of the cycle reflected the time spent by the network in up and down states. The membrane potential distribution during spontaneous activity shows a clear bimodal distribution in all recorded neurons (Figure S4, S7). Input resistance was measured as the slope of a linear fit between injected depolarizing and hyperpolarizing current steps and membrane potential. It has been described that MSNs have a prominent inward membrane rectification at hyperpolarized membrane potentials (Mahon et al., 2004; Nisenbaum and Wilson, 1995). In order to better quantify and measure this rectification we constructed four independent linear functions in response to the negative and positive steps delivered at up or down states. Evoked responses were measured and compared for up and down states. The onset of the evoked sensory responses was calculated as the average time between the stimulus trigger and the onset of the evoked potential of at

least 40 stimuli presented at 0.2 Hz. We used the first and second time derivative of the membrane potential to determine the onset and peak of the sensory response. Response amplitude was defined as the voltage difference between the peak and onset potentials and slopes were obtained as *dv/dt* between the onset and peak time interval. Unless mentioned explicitly, all statistical tests performed were paired or independent student's t-test following the Shapiro-Wilk normality test for all compared data points. Error bars presented in the graphs represent the standard error of the mean (SEM).

Anatomy.

Anterograde tracing. Both sex adult mice were anesthetized with intraperitoneal injection of ketamine and methodomidine, and placed in the stereotaxic as described above. All injections were made with glass pipettes (borosilicate, OD = 1.5 mm, ID = 1.18 mm) with a tip diameter of 5-10 µm. A total of 150–250 nl of BDA 10% (10,000 MW lysine-fixable biotin dextran amine, Molecular Probes) was dissolved in 0.9% NaCl and fast green (to aid visualization of the injected tracer). Injections were performed in layer 5 of BF and V1 using air pressure pulses. A single injection was done for each cortical area and animal using the coordinates described above, as taken from Paxinos and Franklin (2001). Following injection, we sealed the skin with surgical veterinary glue (3M Vetbond Veterinary Tissue Adhesive 1469SB). The analgesic carprofen (Rimadyl; Pfizer) was administered subcutaneously at 5mg/kg, and mice were awakened with intraperitoneal injections of a mixture of atipamezole (Antisedan; Orion Pharma; 1 mg/kg) and naloxone (0.1 mg/kg) diluted in 0.9 % NaCl. Mice were then returned to the animal facilities in separate cages. After 3-6 days animals were transcardially perfused with a solution containing 4 % formalin and 14 % saturated picric acid dissolved in 0.1 M phosphate buffer (PB, pH 7.4). Brains were extracted and stored in this fixative solution for 24-48 hours. Before cutting, brains were transferred into PBS containing 12 % sucrose for 24 hours. Coronal slices (20 µm thick) of both hemispheres containing the entire striatum (from AP 1.7 mm to AP -2.3 mm, following Paxinos and Franklin (2001)) were obtained using a cryostat and collected on gelatin coated slides. Sections were incubated over night with Cy3-conjugated streptavidin (Jackson ImmunoResearch Laboratories) and NeuroTrace 500/525 Green Fluorescent Nissl Stain (Invitrogen) diluted (1:1000) in 1 % BSA, 0.3 % Triton-X 100 in 0.1 M PB. Finally the glass slides were covered with glycerol containing 2.5 % diazabicyclo 2.2.2 octane (Sigma).

Morphological staining. At the end of each experiment the mouse was perfused and the brain was placed in fixative solution for 1-2 hours (same procedures and solution described above). After that, the brain was placed in a 0.01 M PBS and at the day before cutting it was maintained in PBS with 12%

sucrose. 10-12 µm thick coronal slices were obtained from the recorded hemisphere. Sections mounted on gelatin-coated slides were incubated overnight with Cy2-conjugated streptavidin (Jackson ImmunoResearch Laboratories) diluted (1:500) in 1 % BSA, 0.3 % Triton-X 100 in 0.1 M PB. In between all experimental procedures, slices were washed with 0.01 M PBS. We used fluorescent microscopy to find stained neurons. The shortest recording duration for a stained neuron was 24 minutes and the average was 55.44 ± 17.87 minutes (n = 45). Neurons were then reconstructed using a confocal microscope (Zeiss LSM 510 Meta).

Immunohistochemistry. Reconstructed striatal neurons were inmunolabeled for the detection of D_1 dopamine receptors, where we found MSNs that clearly expressed D_1 or not (D_1 n = 15; putative D_2 n = 13). Primary and secondary antibodies were diluted in 1 % BSA, 0.3 % Triton-X 100 in 0.01 M PBS. Sections were incubated between 48-60 hr at 4 °C with primary antibody diluted in 1:500 (D_1): Rat anti-D_1 dopamine receptor (Sigma-Aldrich). This antibody is selective for the 97 amino acid C-terminal fragment of human D_1. Sections were then incubated again for 60 min at room temperature with Cy3-conjugated affiniPure donkey anti-rat IgG (H+L) diluted 1:500 (Jackson Inmuno Research Laboratories). Finally, slides were mounted in glycerol containing an anti-fading agent. The slides were washed in 0.01 PBS at least 3 times for 15 min periods between each procedure step. We used fluorescent and confocal microscopy to recognize the MSN receptor expression (D_1). In order to visualize the results we used pseudo-color to represent the neurobiotin in red and the D_1 receptor expression in green. In order to control for the efficacy of the D_1receptor expression described above we stained slices from D2 EGFP mice, showing that somata of D2 expressing neurons were not stained by the antibody (Figure S5).

Image analysis. Photomicrographs of results were taken with Zeiss Axiocamp (Carl Zeiss AB, Stockholm, Sweden) or an Olympus BX51 (Olympus Sverige AB, Stockhom, Sweden) digital camera. Illustrations were prepared in Adobe Photoshop and Illustrator and images were only adjusted for brightness and contrast. Confocal Z-stacks of the slices were obtained using a Zeiss Laser scanning and mounted using ImageJ (Wayne Rasband, National Institutes of Health, USA).

References for Supplemental Information

Gong, S., Zheng, C., Doughty, M.L., Losos, K., Didkovsky, N., Schambra, U.B., Nowak, N.J., Joyner, A., Leblanc, G., Hatten, M.E.*, et al.* (2003). A gene expression atlas of the central nervous system based on bacterial artificial chromosomes. Nature *425*, 917-925.

Holtmaat, A., Bonhoeffer, T., Chow, D.K., Chuckowree, J., De Paola, V., Hofer, S.B., Hubener, M., Keck, T., Knott, G., Lee, W.C.*, et al.* (2009). Long-term, high-resolution imaging in the mouse neocortex through a chronic cranial window. Nature protocols *4*, 1128-1144.

Mahon, S., Deniau, J.M., and Charpier, S. (2004). Corticostriatal plasticity: life after the depression. Trends in neurosciences *27*, 460-467.
Nisenbaum, E.S., and Wilson, C.J. (1995). Potassium currents responsible for inward and outward rectification in rat neostriatal spiny projection neurons. The Journal of neuroscience : the official journal of the Society for Neuroscience *15*, 4449-4463.
Paxinos, G., and Franklin, K. (2001). The Mouse Brain in Stereotaxic Coordinates, 2nd edn (San-Diego, California: Academic Press).
Reig, R., and Sanchez-Vives, M.V. (2007). Synaptic transmission and plasticity in an active cortical network. PloS one *2*, e670.
Seamari, Y., Narvaez, J.A., Vico, F.J., Lobo, D., and Sanchez-Vives, M.V. (2007). Robust off- and online separation of intracellularly recorded up and down cortical states. PloS one *2*, e888.